Bull. Mater. Sci., Vol. 40, No. 7, December 2017, pp. 1429–1434
https://doi.org/10.1007/s12034-017-1510-1

Temperature-independent photoluminescence response in ZnO:Ce nanophosphor

G L BHAGYALEKSHMI*, A P NEETHU SHA and DEEPTHI N RAJENDRAN
Department of Physics, Govt. College for Women, Vazhuthacaud 695014, India
*Author for correspondence (bhagyalekshmi_gl@yahoo.com)

MS received 11 August 2016; accepted 2 May 2017; published online 6 December 2017

Abstract. A comparative study of structural and luminescence properties of ZnO:Ce^{3+} nanophosphors prepared by combustion method and solid-state reaction method is presented in this study. The powder XRD exhibits hexagonal wurtzite phase and crystallite size falls in the nanometre range. The optical band gap reduction is less in samples synthesized by combustion method. Photoluminescence (PL) spectra of ZnO:Ce excited at near-ultra violet region (325 nm) gives an evidence of its wide range of applications in lighting purposes.

Keywords. Nanophosphor; XRD; hexagonal wurtzite; band gap; photoluminescence; combustion.

1. Introduction

Research on zinc oxide (ZnO) is very intense nowadays, since it is a multifunctional direct wide band gap II–VI semiconductor (∼3.37 eV), which exhibits attractive properties such as large exciton binding energy (60 meV), low refractive index (1.9), resistance to high-energy irradiation, stability to intense ultraviolet (UV) illumination and low toxicity. The nanostructures of ZnO could have been considered for many practical applications in ceramics, piezoelectric transducers, chemical sensors, anti-UV additives, photocatalysts and microwave absorbers, etc. [1–4]. Current attracting application of ZnO is mainly for photoelectric applications, such as UV-light emitters, transparent high power electronics, window materials for display and solar cells, and so on [5–8]. Recently, to improve the electrical, optical and magnetic properties, the ZnO nanostructures are doped with different elements [9–12].

Rare-earth ions with high fluorescent efficiencies and very narrow line fluorescence bands are widely used as activators in different hosts. Rare-earth-doped nanophosphors have optical emissions from the 4f–4f or 4f–5d transition of rare-earth ions. Nowadays, rare-earth-doped ZnO semiconductor is an interesting field of study because of its unique optical properties and promising applications in optoelectronic devices [13–19]. Since cerium oxide (CeO_2) has a band gap of ∼3 eV and shows interesting properties similar to that of ZnO, the doping of Ce has a strong impact on the structural and optical properties of ZnO [20].

Different synthesis routes were developed for the preparation of Ce-doped ZnO nanophosphor [21–26]. The present work discusses the structural and optical properties of Ce-doped ZnO synthesized by combustion method and solid-state reaction method. The prepared nanopowders were characterized by powder X-ray diffraction (XRD), scanning electron microscopy (SEM), Fourier transform infrared spectroscopy (FTIR), UV–visible spectroscopy and photoluminescence spectroscopy (PL).

2. Experimental

All chemicals used for the synthesis are of analytical grade and hence, no further purification is required. Ce-doped ZnO ($Zn_{(1-x)}Ce_xO$ with $x = 1\%$) nanopowders were synthesized by combustion method, using zinc nitrate hexahydrate, $Zn(NO_3)_2 \cdot 6H_2O$ and cerium nitrate hexahydrate, $Ce(NO_3)_3 \cdot 6H_2O$ in the molar ratio of 4:5. Glycine ($C_2H_5NO_2$) is used as fuel for the reaction. Auto ignition takes place and nanocrystalline powders were formed. The prepared samples were annealed at various temperatures for 3 h.

In solid-state reaction method, the ZnO and CeO_2, taken in suitable stoichiometric proportions, were thoroughly mixed in an agate mortar. The mixture was fired in air at 700°C for 3 h. The synthesized nanopowders were used for all characterizations. The structural studies were carried out using XRD analysis by Bruker AXS D8 Advance with Cu target radiation ($\lambda = 1.5406$ Å). FTIR spectra were recorded using IR Prestige-21. The morphology of the particles was studied using SEM (JEOL, JSM-6390LV). To estimate the band gap, optical absorption measurements were performed by UV–visible spectroscopy (UV-2450 spectrophotometer). The PL emission spectra studies were carried out using LS fluorescence spectrometer.

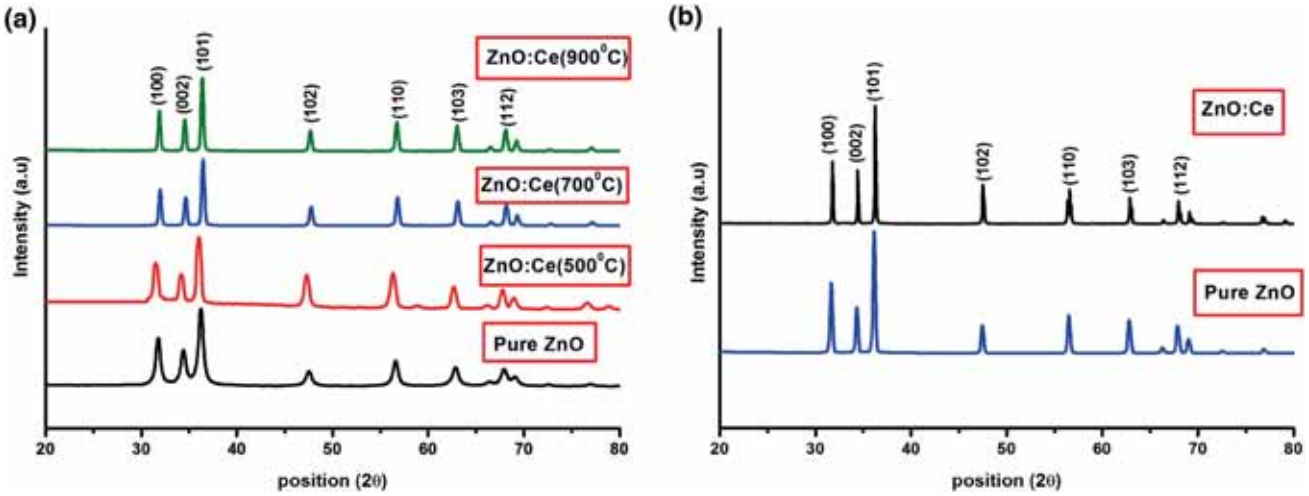

Figure 1. XRD patterns of **(a)** pure ZnO and Ce-doped ZnO nanophosphor (500–900°C) synthesized by combustion synthesis and **(b)** XRD patterns of pure ZnO and Ce-doped ZnO nanophosphor synthesized by solid-state reaction method.

Table 1. Crystallographic parameters obtained from undoped and Ce-doped ZnO nanophosphors.

		d spacing (Å)			Lattice parameters				
Method of preparation	Sample details	100	002	101	*a*	*c*	*c*/*a*	Cell volume, *V* (Å)	*D* (nm)
Combustion synthesis	Pure ZnO	2.81	2.60	2.47	3.24	5.20	1.6049	47.6616	39.0934
	$Ce_{0.01}:Zn_{0.99}O$ (500°C)	2.84	2.62	2.49	3.28	5.16	1.5731	48.0745	19.4209
	$Ce_{0.01}:Zn_{0.99}O$ (700°C)	2.80	2.58	2.46	3.24	5.14	1.5864	46.7273	23.2374
	$Ce_{0.01}:Zn_{0.99}O$ (900°C)	2.80	2.59	2.46	3.23	5.13	1.5882	46.3489	26.1362
Solid-state reaction	Pure ZnO	2.82	2.61	2.48	3.26	5.25	1.625	48.3183	29.6375
	$Ce_{0.01}:Zn_{0.99}O$	2.81	2.72	2.47	3.24	5.16	1.592	46.9091	43.9939

3. Result and discussion

3.1 *Structural properties*

XRD pattern of ZnO:Ce nanophosphor by combustion method (figure 1a) and solid-state reaction method (figure 1b) exhibits hexagonal wurtzite structure. Intense diffraction peaks of the ZnO were indexed after comparing them with the data in the JCPDS file 1314-13-2. All the diffraction lines correspond to the standard Bragg positions of hexagonal wurtzite ZnO with space group P63mc. There is no additional diffraction peaks in Ce-doped ZnO samples, which indicates the successful incorporation of cerium ions on the ZnO surface.

The crystallite size of all synthesized samples was estimated by applying the Scherrer equation [27]. The crystallite size of Ce-doped ZnO nanoparticles prepared by combustion synthesis was in the range of 19–26 nm, while in solid-state method, it was found to be 43 nm. In combustion method, crystallite size increases with annealing temperature. Heating process enhances number of collisions between particles, which leads to the coalesce with one another to form a larger particle [28,29]. Crystallographic parameters obtained from XRD are included in table 1.

Microstructural characterization and topography of the synthesized samples were carried out by SEM analysis. SEM image of the Ce-doped ZnO nanophosphor by combustion method appears like agglomerated with voids and pores. Porosity may be attributed to the liberation of large amount of gaseous products like H_2O vapours, CO_2 and N_2 during combustion process (figure 2a–c). Whereas, the Ce-doped ZnO nanophosphor by solid-state reaction method showed the rough and tough morphology. It is also clear that the synthesized sample consists of irregular micro-slabs (figure 2d).

Chemical and structural changes of synthesized nanomaterials can be investigated by FTIR spectroscopic analysis. The FTIR spectra of Ce-doped ZnO nanophosphor in the region of 400–4000 cm^{-1} prepared by combustion and solid-state reaction methods are shown in figure 3. The spectra shows the band located at around 450–490 cm^{-1} can be attributed to the Zn–O stretching mode in the ZnO lattice [30]. Peak observed at 913 cm^{-1} may be due to the presence

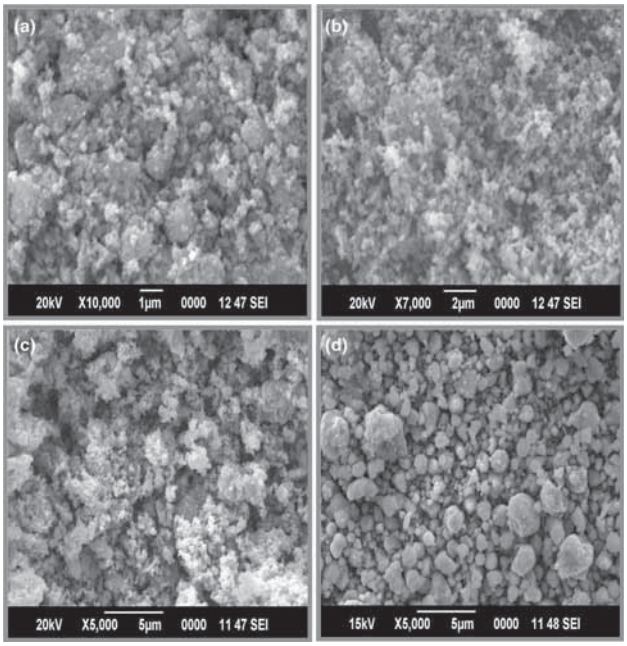

Figure 2. **(a–c)** SEM image of Ce-doped ZnO nanophosphor synthesized by combustion synthesis annealed at different temperatures 500–900°C and (**d**) SEM image of Ce-doped ZnO nanophosphor synthesized by solid-state reaction method.

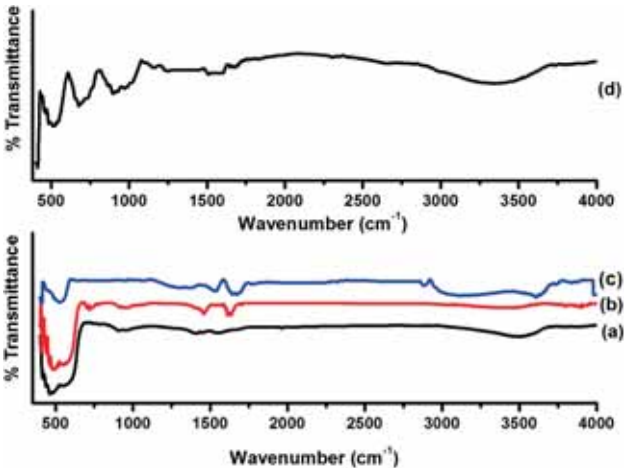

Figure 3. **(a–c)** FTIR spectra of Ce-doped ZnO nanophosphor synthesized by combustion synthesis annealed at different temperatures 500–900°C and **(d)** FTIR spectra of Ce-doped ZnO nanophosphor synthesized by solid-state reaction method.

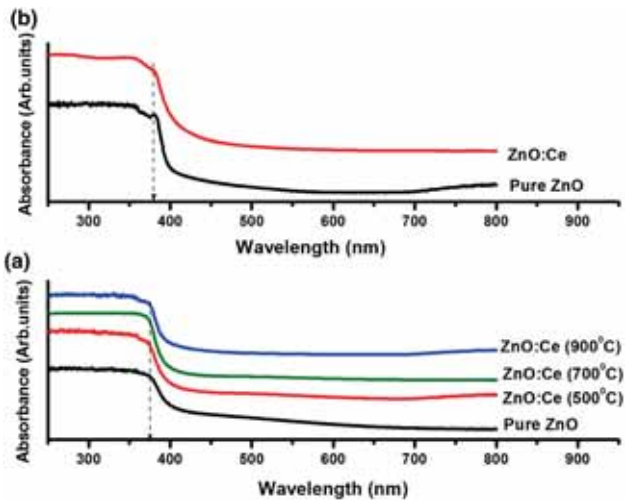

Figure 4. Absorbance spectra of **(a)** pure ZnO and Ce-doped ZnO nanophosphor (500–900°C) synthesized by combustion synthesis and **(b)** absorbance spectra of pure ZnO and Ce-doped ZnO nanophosphor synthesized by solid-state reaction method.

of Ce–O stretching vibration [31]. Some additional peaks were observed in the FTIR spectra of the samples prepared by combustion method (figure 3a–c). The broad absorption peak centred at 3521 and 1595 cm^{-1} assigned to O–H stretching vibrations [32]. Intense peak at 1381 cm^{-1} due to stretching vibrations of C=O bond. It is observed that the area of hydroxial peak diminishes with rise in temperature. Peak at 1369 cm^{-1} corresponds to C=O bending vibrations and will diminish at higher annealed temperature. These peaks were absent in the FTIR spectra of the sample prepared by solid-state reaction method (figure 3d).

3.2 *Optical properties*

Absorbance spectra of pure and Ce-doped ZnO samples, prepared by combustion and solid-state reaction method, are demonstrated in figure 4. The excitonic absorption peak of prepared samples by both methods lies in the region of 250–350 nm, which is fairly blue shifted from the absorption edge (i.e., much below the band gap wavelength of 365 nm, $E_g = 3.4$ eV) of bulk ZnO. The energy band gap of the material is estimated with absorbance and photon energy, given by Wood and Tauc's relation.

$$\alpha = A\left(h\nu - E_g\right)^n. \quad (1)$$

The value of band gap was determined by plotting $(\alpha h\nu)^2$ *vs.* $h\nu$. Band gap studies reveal that optical band gap undergoes a reduction with increasing temperature in combustion synthesis (figure 5a). In solid-state reaction method (figure 5b), band gap undergoes a reduction with doping. Decrease in band gap may be ascribed to the fact that new defects are introduced after substitution of Ce by Zn atoms to electronegativity and ionic radius difference between Zn and Ce. Dopant atoms take up the energy levels located in the bottom of the conduction band. The valence electrons require extra energy to be excited to higher energy states in the conduction band. It weakens the electron and hole-wave functions, which result from the reduction of quantum size effect and enhancement of crystallinity accompanied with increase in particle size. Increase in band

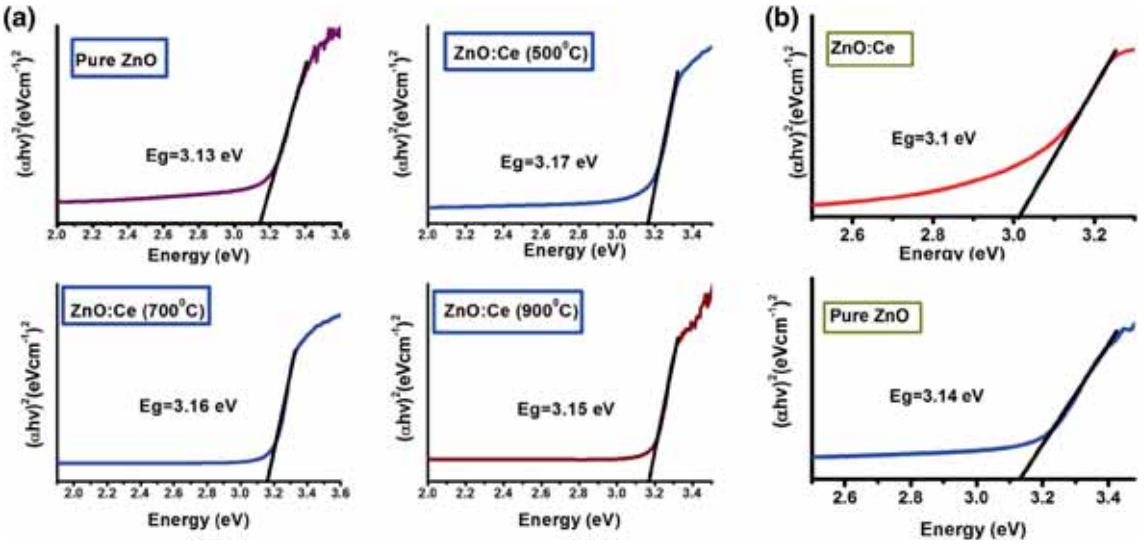

Figure 5. Tauc plot of **(a)** pure ZnO and Ce-doped ZnO nanophosphor (500–900°C) synthesized by combustion synthesis and **(b)** Tauc plot of pure ZnO and Ce-doped ZnO nanophosphor synthesized by solid-state reaction method.

Table 2. Band gap values of undoped and Ce-doped ZnO nanophosphors.

Method of preparation	Sample details	Band gap, E_g (eV)
Combustion synthesis	Pure ZnO	3.13
	$Ce_{0.01}$:$Zn_{0.99}O$ (500°C)	3.17
	$Ce_{0.01}$:$Zn_{0.99}O$ (700°C)	3.16
	$Ce_{0.01}$:$Zn_{0.99}O$ (900°C)	3.15
Solid-state reaction method	Pure ZnO	3.14
	$Ce_{0.01}$:$Zn_{0.99}O$	3.1

gap attributed to quantum confinement theory. Spatially confined electrons and holes undergo an optical transition from the valence to conduction band, which will increase in energy, effectively increasing the band gap (E_g) [33]. Calculated values of band gap and crystallite size are shown in table 2.

PL emission spectra of pure and Ce-doped ZnO nanophosphors synthesized by combustion synthesis and solid-state reaction method were recorded under excitation of 325 nm as shown in figure 6. Spectrum exhibit a sharp UV peak and four visible peaks. The intense UV peak corresponding to near-band edge emission of ZnO originating from electron–hole recombination [34]. The broad emission spectrum in visible region is the result of sum of peaks centred at 420, 457 and 486 and 538 nm. The peak at 457 nm may due to the transitions from $^2D_{3/2}$–$^2F_{7/2}$ state. The blue emission at 457 and 487 nm may be due to singly occupied oxygen vacancies in deep trapped holes. Peak at 420 nm may be due to Zn vacancies [35]. Peak in green region correspond to deep-level or trap-state emission from $^5D_0$–$^7F_0$ [36,37]. Vanheusden *et al* [38] reported that green luminescence in ZnO may be due to the presence of singly ionized oxygen vacancies. In

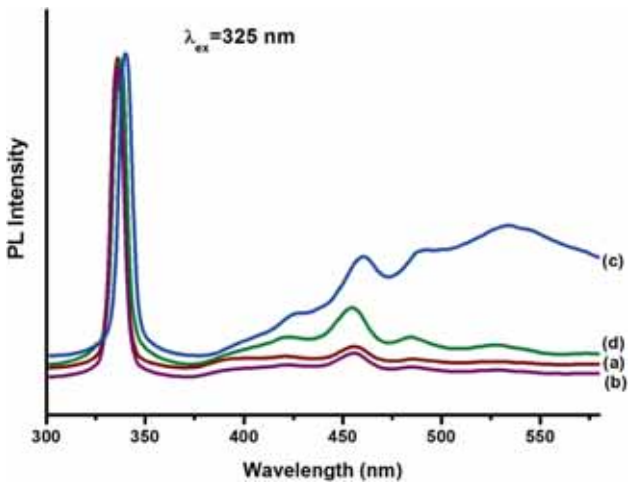

Figure 6. Emission spectra of (a) pure ZnO, (b) Ce-doped ZnO nanophosphor synthesized by combustion synthesis and (c) pure ZnO, (d) Ce-doped ZnO nanophosphor synthesized by solid-state reaction method.

combustion method, most prominent emission of pure and Ce-doped samples lies in blue region. It is seen that pure ZnO

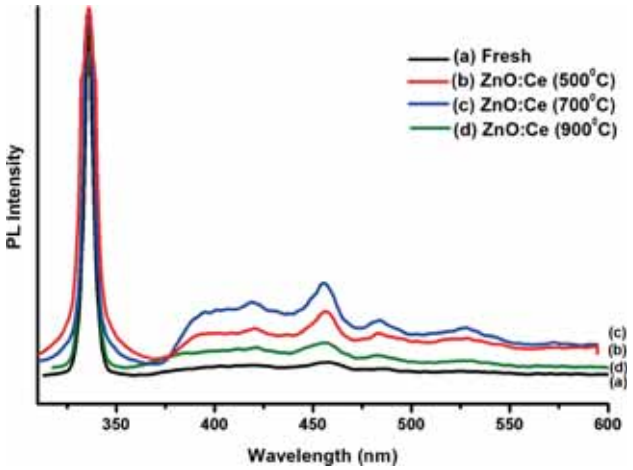

Figure 7. Effect of annealing on emission spectra of Ce-doped ZnO phosphor by combustion synthesis method.

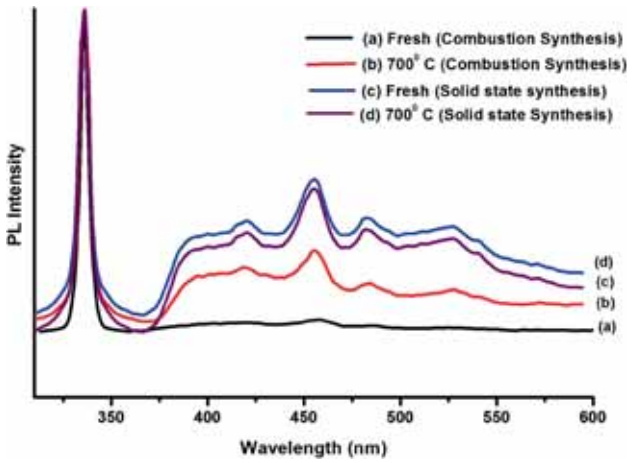

Figure 8. Comparison of emission spectra of Ce-doped ZnO phosphor by (a) combustion synthesis as prepared, (b) combustion synthesis (annealed), (c) solid-state reaction as prepared and (d) solid-state reaction (annealed).

sample prepared by solid-state reaction method favours green emission. On Ce doping into ZnO nanoparticle, it shifts the most intense emission from green to blue region. Different emission in two methods may due to quantum confinement effect. The particles reaching in nanoscale dimension makes energy levels discrete and increases or widens up the band gap, which makes greater optical transition energy in confined systems.

To understand the effect of annealing on emission spectra of Ce-doped ZnO phosphor prepared by combustion synthesis, PL spectra were recorded after annealing the synthesized sample at 500, 700 and 900°C (figure 7). Luminescence intensity of most prominent peak becomes higher after post annealing treatment of Ce-doped ZnO phosphor up to 700°C and then it diminishes. Heat treatment also affects the crystallinity and phase of the prepared samples. Crystalline behaviour of the Ce-doped ZnO nanophosphor increases with annealing temperature. At high temperature, luminescence quenching ascribed to the movement of oxygen and zinc atoms from interstitial to lattice sites [39].

By comparing the emission spectra of solid state and combustion synthesis, both samples are prepared at the same thermal conditions. Absolute emission intensity of Ce-doped ZnO phosphor prepared by solid state reaction method is more than that of sample prepared by combustion synthesis as shown in figure 8. There is no effect of annealing on the luminescence behaviour of Ce-doped ZnO nanophosphor prepared by solid state reaction method. Post heat treatment in combustion method increases the PL intensity of most prominent peak first then at high temperature it diminishes, while in solid-state reaction method PL intensity is unaffected by the temperature. Therefore, solid-state reaction method is capable of producing phosphor material without providing further heat treatment.

4. Conclusion

Structural, morphological and optical properties of Ce-doped ZnO nanophosphor prepared by combustion synthesis and solid-state reaction method were studied. Post-annealing temperature intensifies the emission and modulate the emission wavelength up to a certain temperature range in combustion method. In solid-state reaction method luminous intensity is unaffected by annealing temperature. For the production of phosphor in single-step, solid state is most applicable method for various display applications.

Acknowledgements

We are grateful to NIIST, Trivandrum and STIC, Cochin, for providing facilities for the analysis of the prepared samples.

References

[1] Gouvêa C A K, Wypych F, Moraes S G, Durán N and Peralta-Zamora P 2000 *Chemosphere* **427** 40
[2] Look D C 2001 *Mater. Sci. Eng.* **383** B80
[3] Park S, Lee D W, Lee J C and Lee J H 2003 *J. Am. Ceram. Soc.* **1508** 86
[4] Zhou Z W, Chu L S and Hu S C 2006 *Mater. Sci. Eng.* **93** B126
[5] Cao H, Xu J Y, Zhang D Z, Chang S H, Ho S T and Seeling E W 2000 *Phys. Rev. Lett.* **5584** 84
[6] Zhang B P, Binh N T, Wakatsuki H, Kashiwaba Y and Haga K 2004 *Nanotechnology* **S382** 15
[7] Ohshima E, Ogino H, Niikura I, Maeda K, Sato M, Ito M *et al* 2004 *J. Cryst. Growth* **166** 260
[8] Pearton S J, Norton D P, Ip K, Heo Y W and Steine T 2005 *Prog. Mater. Sci.* **293** 50
[9] Lee W, Jeong M C and Myoung J M 2004 *Appl. Phys. Lett.* **85** 6167

[10] Yuan G D, Zhang W J, Jie J Sh, Fan X, Tang J X, Lee Ch S *et al* 2008 *Adv. Mater.* **20** 168
[11] Mahmoud W E, Al-Ghamdi A A, El-Tantawy F and Al-Heniti S 2009 *J. Alloys Compd.* **59** 485
[12] Seetawan U, Jugsujinda S, Seetawan T, Ratchasin A, Euvananont C, Junin C *et al* 2011 *Mater. Sci. Appl.* **2** 1302
[13] Shi H X, Zhang T Y and Wang H L 2011 *J. Rare Earth* **29** 746
[14] Zeng R, Wang J G, Cui J Y, Hu L and Mu K G 2010 *J. Rare Earth* **28** 353
[15] Fan C M, Xue P and Sun Y P 2006 *J. Rare Earth* **24** 309
[16] Bian L, Song M X, Zhou T L, Zhou X Y and Dai Q Q 2009 *J. Rare Earth* **27** 461
[17] Zalaj M 2014 *J. Rare Earth* **32** 487
[18] Li X Z, Hu Z L, Zhao X B and Lu X W 2013 *J. Rare Earth* **31** 1157
[19] Du J, Li B H, Huang J J, Zhang W L, Peng H L and Zou J G 2013 *J. Rare Earth* **31** 992
[20] Yang J H, Gao M, Wang Y X and Fan H G 2008 *Appl. Surf. Sci.* **255** 2646
[21] John J S, Coffer J L, Chen Y and Pinizzotto R F 2000 *Appl. Phys. Lett.* **77** 1635
[22] Bubendorff J L, Ebothe J, El Hichou A, Dounia R and Addou M 2006 *J. Appl. Phys.* **100** 14505
[23] Alaoui Lamrani M, Addou M, Soofiani Z, Sahraoui B, Ebothé J, El Hichou A *et al* 2007 *Opt. Commun.* **277** 196
[24] Sofiani Z, Bouchta S and Addou M 2007 *J. Appl. Phys.* **101** 63104
[25] Mais N, Reithmaier J P, Forchel A, Kohls M, Spanhel L and Müller G 2005 *Appl. Phys. Lett.* **75** 1999
[26] Liu Y, Yang Q and Xu C 2008 *J. Appl. Phys.* **104** 64701
[27] Kumbhakar P and Singh D 2008 *Chalcogen. Lett.* **5** 387
[28] Iqbal M Z, Ali S and Mirza M A 2008 *CODEN JNSMAC* **48** 11
[29] Kenevey K, Valdivieso F, Soustelle M and Pijolat M 2001 *Appl. Catal. B: Environ.* **29** 93
[30] Sudheesh K, Shukla, Agorku E S, Mittal H and Mishra A K 2014 *Chem. Papers* **68** 217
[31] Harish Kumar and Rani R 2013 *Int. Lett. Chem. Phys. Chem. Astron.* **14** 26
[32] Varughese G, Jithin P W and Usha K T 2015 *Phys. Sci. Int. J.* **5** 146
[33] Ahmad M, Ahmed E, Zafar F, Khalid N R, Niaz N A, Hafeez A *et al* 2015 *J. Rare Earth* **33** 255
[34] Beche E, Charvin P, Perarnau D, Abanades S and Flamant G 2008 *Surf. Interf. Anal.* **40** 264
[35] Jayachandraiah C, Krishnaiah G and Siva Kumar K 2014 *Int. J. Chem. Tech. Res.* **6** 3378
[36] Nitin K, Adam D and Jong-In H 2005 *J. Nanosci. Nanotechnol.* **5** 1915
[37] Bagnall D M, Chen Y F, Shen M Y, Zhu Z, Goto T and Yao T 1998 *J. Cryst. Growth* **184** 605
[38] Vanheusden K, Seager C H, Warren W L, Tallent D R and Voig J A 1996 *J. Appl. Phys.* **79** 7983
[39] Vishwas N, Rao M K, Gowda K V A and Chakradhar R P S 2010 *Spectrochim. Acta: Part A* **77** 330